Optimization and Modelling of Resistance Spot Welding Process Parameters for Quality Improvement Using Taguchi Method and Artificial Neural Network

Imtiaz Ali Soomro[1,2,*], Srinivasa Rao Pedapati[1], Mokhtar Awang[1], Afzal Ahmed Soomro[1], Mohammad Azad Alam[1], Bilawal Ahmed Bhayo[1,3]

* *imtiaz_17007503@utp.edu.my*

[1] Department of Mechanical Engineering, University Technology PETRONAS, Seri Iskandar, 32610, Perak Darul Ridzuan, Malaysia

[2] Department of Metallurgy and Materials Engineering, Mehran University of Engineering and Technology, Jamshoro 76062, Sindh, Pakistan

[3] Department of Mechanical Engineering, Mehran University of Engineering & Technology SZAB Campus Khairpur Mir's, Sindh, Pakistan

Abstract: This paper investigated the optimization, modeling, and effect of welding parameters on the tensile shear load-bearing capacity of double pulse resistance spot-welded DP590 steel. Optimization of welding parameters was performed using the Taguchi design of experiment method. A relationship between input welding parameters i.e., second pulse welding current, second pulse welding current time, and first pulse holding time and output response i.e, tensile shear peak load was established using regression and neural network. Results showed that the maximum average tensile shear peak load of 26.47 was achieved at optimum welding parameters i.e., second pulse welding current of 7.5 kA, second pulse welding time of 560 ms, and first pulse holding time of 400 ms. It was also found that the ANN model predicted the tensile shear load with higher accuracy than the regression model.

Keywords: Resistance spot welding, Taguchi method, Artificial neural network, Regression model, Tensile shear load.

1. INTRODUCTION

Dual-phase (DP) steels are a type of advanced high-strength steel (AHSS) that exhibits high strength and ductility. The combination of these outstanding mechanical properties is attributable to two-phase microstructure DP steels, which consist of a soft ferrite embedded with hard martensite [1]. Resistance spot welding (RSW) is the most commonly utilized welding technology for joining vehicle components. A typical modern vehicle has several thousand spot welds. The ability of a vehicle structure to protect its passengers from injury in the event of a collision is heavily reliant on the integrity and mechanical performance of spot welds. A spot weld acts as a fold initiator during a collision, transmitting load to automobile assembly. Therefore, the quality of the resistance spot welds in terms of mechanical performance is crucial to the overall integrity and reliability of a vehicle [2].

The most common problem encountered in resistance spot welds of automotive steels is interfacial failure (IF) or partial interfacial failure (PI) combined with the reduced mechanical performance of the welded joint. During RSW, the liquid metal cools at a rate of roughly 105°C/s; due to this high cooling rate, a hard and brittle martensite structure is produced in the weld nugget [3]. This hardened microstructure in the nugget causes an interfacial failure which allows crack propagation through the weld centerline and diminishes the mechanical performance of the welded joint, particularly in terms of load bearing and energy absorption capacity. Tempering the martensitic structure is essential to suppress brittle interfacial fracture. Postweld tempering via applying a secondary pulse current after the primary/first melting pulse current can alleviate the risk of high sensitivity to interfacial fracture [4]. Although some studies [3-5] have been carried out to explore double pulse RSW of high-strength steels, a closer look at the literature reveals several gaps and shortcomings, including defining the optimum set of secondary pulse welding process parameters because the slightest change in the material composition and sheet thickness influences the selection of optimum

Imtiaz Ali Soomro, Srinivasa Rao Pedapati, Mokhtar Awang, Afzal Ahmed Soomro, Mohammad Azad Alam, Bilawal Ahmed Bhayo

process parameters. The success of the postweld tempering treatment is highly dependent on precisely controlling the amount of heat input, which is influenced by the secondary pulse welding current, secondary pulse welding time, and electrode holding time between primary and secondary pulses. Identifying the optimal welding conditions for achieving the desired weld quality through trial and error is costly and time-consuming. As a result, a precise modeling technique for forecasting weld quality is necessary, thus saving time and resources.

Taguchi design of experiment (DOE) method has gained popularity recently due to its robust approach to optimizing the welding process parameters [6, 7]. In this method, the parameters that influence process outcome(s) are placed in different rows of a constructed orthogonal array (OA), and the experiments are carried out in line with the OA. Taguchi's method adopts fractional factorial rather than full factorial, allowing for the simple creation of experimental trials with a large number of factors that vary on a few levels. The mean and variance of the response are then combined to form a single performance metric known as the signal-to-noise (S/N) ratio [8]. Taguchi's DOE method has numerous advantages; however, when used in practice, the method has some limitations. When the given parameters are continuous, the Taguchi technique is unable to determine the actual optimal values because it only addresses discrete parameters. Artificial neural networks (ANN) are one of the most commonly used modeling techniques for predicting output responses even with continuous parameters. The ANN technique with a nonlinear function can accurately represent the complex relationship between inputs and outputs [9]. The use of ANN in the modeling of manufacturing processes has grown in recent years, owing to its ability to extract the necessary information from the input data. The use of ANN in the welding process, in particular, has been an enormous success. Bharathi Kannan et al. [10] employed ANN successfully to obtain the optimal laser welding parameters for 1 mm thick NiTinol sheets. Arunchai et al. [11] used ANN to find the optimum parameters for maximum tensile shear strength of resistance spot welded dissimilar thickness aluminum alloy. Babu et al. [12] carried out parameter optimization using ANN of friction stir welding of cryo-rolled aluminum alloy to obtain weld joints with maximum strength. Although using ANNs allows for the development of high-performance models, determining the appropriate training and architectural parameters of an ANN remains a difficult task. These parameters are typically determined through a trial and error-procedure. According to the authors' knowledge, no previous works define the ANN or regression model development to predict the spot weld joint strength made via double pulse RSW. The present study aims to develop regression and ANN models using a novel method i.e., based on Taguchi-optimized data to ensure the best weld quality in terms of maximum tensile shear load carrying capacity.

2. MATERIALS CHARACTERIZATION

In the present investigation, galvanized dual-phase (DP590) steel sheet is used. The chemical composition of the steel was determined using an optical spark emission spectrometer. The composition (wt %) of the DP590 steel is C (0.099), Mn (1.70), Si (0.388), S (0.007), Al (0.0301), and the remaining is Fe. The tensile strength, yield strength, and ductility of DP590 steel are 694 MPa, 440 MPa, and 11.58%, respectively. Fig. 1 depicts the microstructure of as received condition steel. DP590 steel sheets with a thickness of 1.8 mm were cut into 40 x 125 mm strips and then overlap-spot welded. The geometry and dimensions of the lap shear tensile specimen are shown in Fig. 2.

Resistance spot welding was performed using a high-frequency alternating-current type semi-automatic welding machine. Truncated cone-shaped copper-alloy electrodes with an 8 mm face diameter were used for welding. A double pulse welding (DPW) schedule was employed for making spot welds. The DPW schedule consists of two cycles i.e. melting pulse cycle (MPC) and plus post-weld heating cycle (PWHC). Fig. 3 shows the schematic illustration of the welding scheme used in the present investigation. The aim of MPC is to produce a target nugget size following $D= 5\sqrt{t}$ (where t is sheet thickness and D is the width of weld nugget) criterion. The aim of PWHC is to reheat the weld to alter the microstructure and decrease the brittleness of the weld nugget.
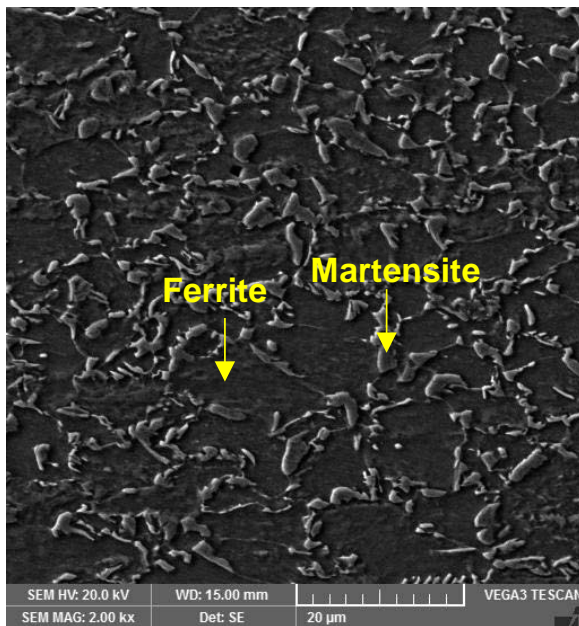
Fig. 1. SEM micrograph exhibiting microstructure of DP590 steel

Table 1 shows the detailed parameters and levels of the double pulse RSW.

Tensile shear peak load is considered as the output/quality characteristic while secondary pulse welding current, secondary pulse welding time, and primary/first pulse holding time are chosen as input process parameters. From a previous study [14], it is found that the secondary

pulse welding current and welding time control the amount of heat supplied to the welding zone, while the 1st pulse holding time influence the cooling rate of the weld zone.
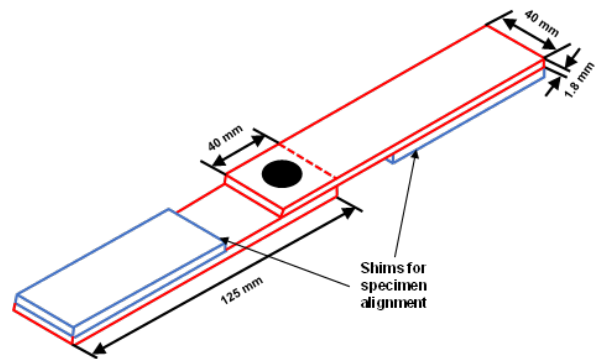

Fig. 2. Geometry and dimension of lap shear tensile specimen

Table 1. Parameters and their levels used for double pulse RSW

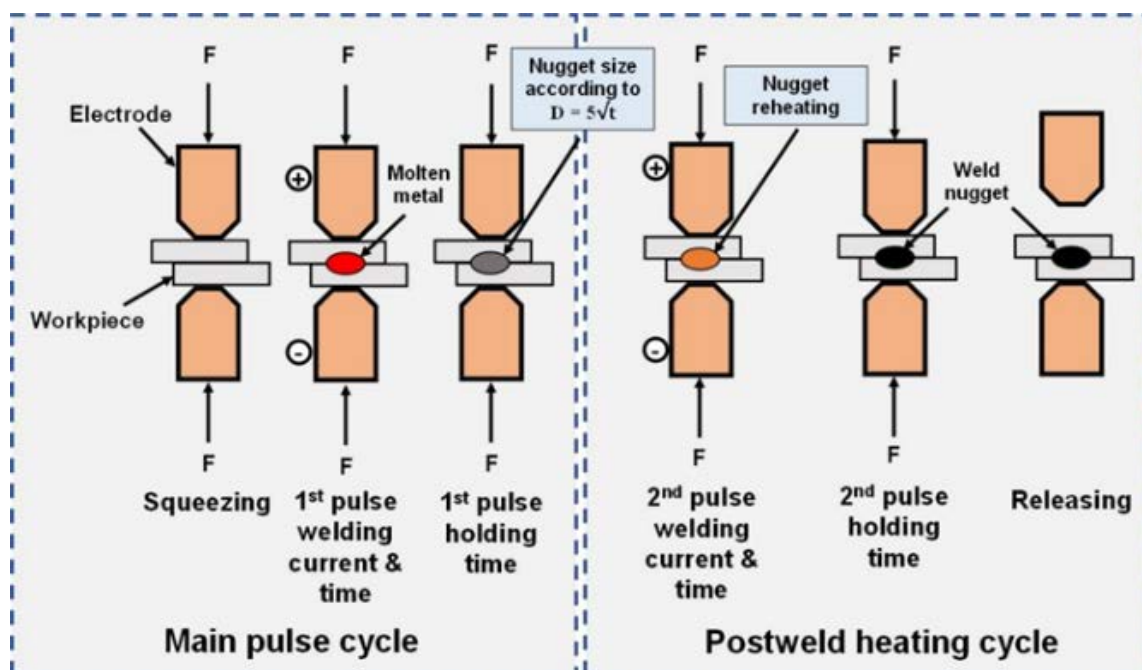| Electrode force (kN)	4
Squeeze time (ms)	500
1st pulse welding current (kA)	7.5
1st pulse welding time (ms)	560
1st pulse holding time (ms)	400, 460, 520, 580
2nd pulse current (kA)	3, 4.5, 6, 7.5
2nd pulse welding time (ms)	140, 280, 420, 580
2nd pulse holding time (ms)	600

Fig. 3. Schematic illustration of double pulse RSW

Imtiaz Ali Soomro, Srinivasa Rao Pedapati, Mokhtar Awang, Afzal Ahmed Soomro, Mohammad Azad Alam, Bilawal Ahmed Bhayo

Based on the significant influence on the weld thermal cycle, three input process parameters are selected. Table 2 shows the selected input process parameters and their levels.

Taguchi method was used to design the experiments. An L16 OA was chosen, and all experiments were carried out according to the designed arrays. Taguchi's L16 OA was chosen based on the degrees of freedom (DOF). In Taguchi's OA design, the degrees of freedom of each factor are equal to n-1, where n is the total number of levels. The DOF of each factor is three (no. of levels minus one i.e., 4-1= 3), and the total DOF is 2 × 4= 8. The total DOF of OA should be greater than or equal to the total DOF of the factors [13]. The total DOF of L16 OA is fifteen (i.e., 16-1= 15); thus, the selected OA is suitable for the investigation and capable of providing full statistical evidence of all the parameters that affect the quality. Table 3 shows the layout of the L16 OA and the arrangement of parameters assigned to each column.

After completing RSW experiments, quasi-static tensile shear tests were performed using a servohydraulic universal testing machine (model: Amsler HA50 Zwick Roell GmbH & Co, KG, Germany) at a cross-head speed of 10 mm/min. The tensile shear peak load was recorded from load-displacement plots of specimens. Two replications are used for each experimental run corresponding to each row of the L16 OA. For microstructural examination, specimens were cut from the center of the welded joints and prepared following standard metallographic methods. The microstructure was examined using scanning electron microscopy (SEM) (model: TESCAN VEGA3, Czech Republic).

3. RESULTS AND DISCUSSION

3.1. Evaluation of Tensile Shear Load

Experimental, regression and ANN-predicted results of the tensile shear test are given in Table 4. Experimental load-displacement plots of all specimens are shown in supplementary Fig. S-1. The highest average tensile shear peak load of 26.46 kN is attained by specimen W16, while the lowest average tensile shear peak load of 23.79 kN is attained by specimen W1.

Fig.4 depicts the failure mode of all specimens, which can be easily distinguished by the appearance of their fractures. Specimens failed in four different ways: interfacial failure (IF), partial-interfacial failure (PIF), pullout failure (PF), and partial-thickness-partial pullout failure (PTPPF). In IF mode, the crack initiated from the notch present at the sheet-sheet interface and propagated rapidly through the center of a nugget. In PIF mode, the fracture first propagated in the nugget at approximately 45o to the surface plane and then redirected through the thickness direction.

The shear stress at the interface of the two sheets controlled the failure in the IF and PIF modes. In PF mode, the nugget is pulled out from one sheet. In PTPPF mode, a slant crack first propagated into the nugget before being redirected through the sheet in the thickness direction, resulting in the removal of some parts of the mating sheet. The tensile stress around the nugget governed the occurrence of failure in the PF and PTPPF modes [14]. Specimens failed via pullout failure exhibit high tensile-shear load-bearing capacity, strength, and ductility, and thus are considered good welds.

Table 2. Welding parameters and their levels considered for double pulse RSW

Parameters	Symbol	Levels			
		1	2	3	4
Secondary pulse welding current (kA)	A	3	4.5	6	7.5
Secondary pulse welding time (ms)	B	140	280	420	560
Primary/first pulse holding time (ms)	C	400	460	520	580

Table 3. DOE based on Taguchi L16 OA

Parameter	Experiment run															
	W1	W2	W3	W4	W5	W6	W7	W8	W9	W10	W11	W12	W13	W14	W15	W16
A	3	3	3	3	4.5	4.5	4.5	4.5	6	6	6	6	7.5	7.5	7.5	7.5
B	140	280	420	560	140	280	420	560	140	280	420	560	140	280	420	560
C	400	460	520	580	460	400	580	520	520	580	400	460	580	520	460	400

Table 4. Experimental, regression and ANN predicted results of tensile shear load

| Experiment No	Input Parameters			Output (Tensile shear peak load)				
	A (kA)	B (ms)	C (ms)	Experimental		Average of Test 1 & Test 2 (kN)	Regression predicted (kN)	ANN predicted (kN)
				Test 1 (kN)	Test 2 (kN)			
W1	3.0	140	400	23.84	23.82	23.83	24.00	23.59
W2	3.0	280	460	23.93	23.91	23.92	23.80	23.56
W3	3.0	420	520	23.77	23.61	23.69	23.80	23.61
W4	3.0	560	580	23.76	23.78	23.77	24.00	23.77
W5	4.5	140	460	23.79	23.89	23.84	23.66	24.07
W6	4.5	280	400	23.89	24.51	24.20	24.37	24.14
W7	4.5	420	580	24.54	25.46	25.00	24.89	24.89
W8	4.5	560	520	25.76	26.16	25.96	25.64	25.74
W9	6.0	140	520	23.85	23.89	23.87	24.06	23.86
W10	6.0	280	580	25.41	25.75	25.58	25.31	25.46
W11	6.0	420	400	25.28	26.32	25.80	25.24	25.80
W12	6.0	560	460	26.39	26.03	26.21	26.55	26.19
W13	7.5	140	580	24.54	25.54	25.04	25.24	25.07
W14	7.5	280	520	26.04	26.06	26.05	25.92	25.89
W15	7.5	420	460	26.34	26.22	26.28	26.39	26.24
W16	7.5	560	400	26.38	26.56	26.47	26.65	26.09
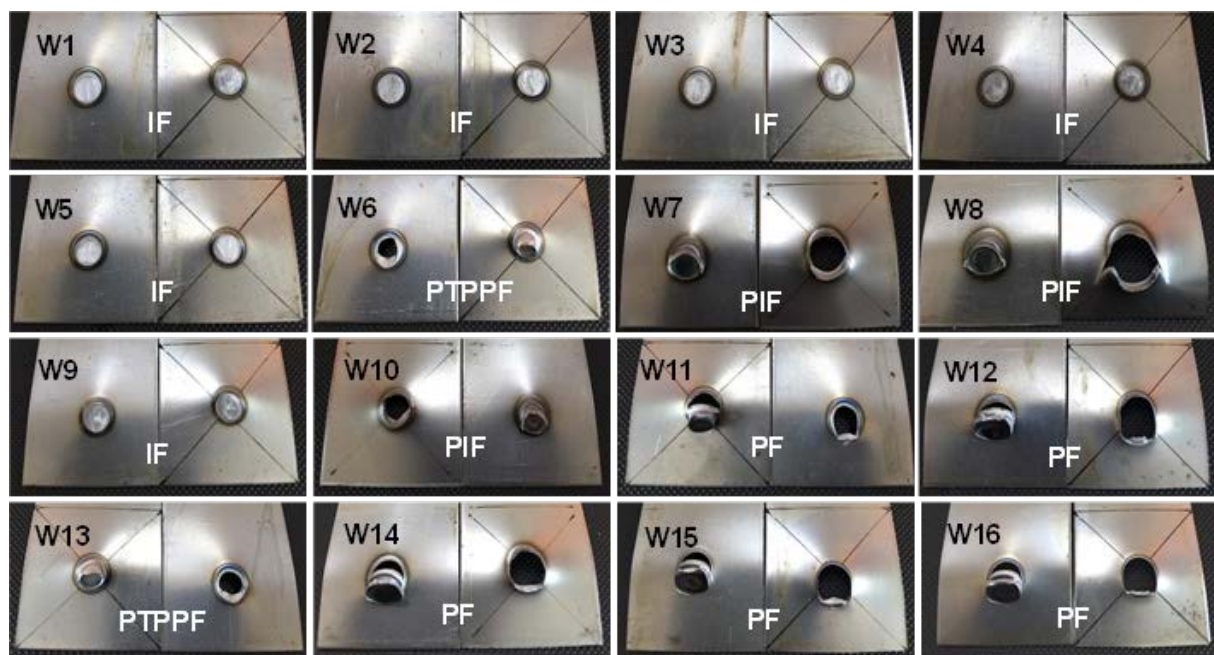
Fig. 4. Photographs showing the failure mode of welds

3.2. Metallurgical Studies

The nugget size is the key factor in determining the quality of spot welds because it determines the failure mode of the weld. In general, the failure mode shifts from interfacial to pullout above a critical nugget size [15]. In order to obtain PF mode in resistance spot welded automotive steels, some industrial standards American Welding Society (D8.9M) define the equation for the critical nugget diameter as D= $4t^{0.5}$ (where t is

sheet thickness), whereas the Japanese Industrial Standard (JIS Z3140) endorses a critical nugget size based on D= $5t^{0.5}$. In the present study, although welds are produced with critical nugget diameter according to D= $5t^{0.5}$ criterion, specimens W1, W2, W3, W4, W5, and W9 failed in the IF mode, which indicates that conventional nugget size criteria merely based on sheet thickness do not guarantee PF mode in DP590 steel resistance spot welds. This is because these

Imtiaz Ali Soomro, Srinivasa Rao Pedapati, Mokhtar Awang, Afzal Ahmed Soomro, Mohammad Azad Alam, Bilawal Ahmed Bhayo

standards presume uniform mechanical properties across the weldment and do not account for the effect of metallurgical variations. Therefore, it is important to analyze the metallurgical aspects of the welds in detail. Macrostructures and nugget size of welded joints are shown in supplementary Fig. S2 and Fig. S3, respectively. Fig. 5 shows the microstructure of the nugget zone of the specimens W1, W7, W13, and W16 failed via IF, PIF, PTPPF, and PF modes, respectively. As can be seen, the nugget microstructure of specimen W1 consists of a fully martensitic structure. The low secondary pulse welding current and low secondary welding time produced insufficient heat to temper the brittle martensite, thus, the weld failed via interfacial failure and exhibited the worst load-bearing capacity and apparent lowest tensile shear peak load.
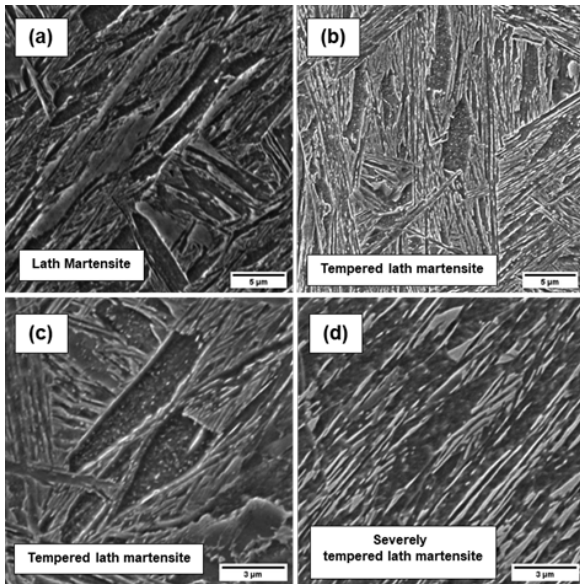

Fig. 5. Microstructure of nugget zone of the welds (a) specimen W1 (b) specimen W7 (c) specimen W13 and (d) specimen W16.

On the other hand, the nugget microstructure of specimens W7, W13, and W16 exhibits a tempered martensite structure. This is because as the secondary pulse welding current and secondary pulse welding time increased, the heat input into the weld nugget increased which in turn intensified the martensite tempering. Moreover, as the electrode holding time between the primary pulse and secondary pulse is decreased, the cooling rate of the weld decreases, and some amount of heat is retained in the weld which is supplemented by total heat input to the nugget

during tempering treatment. It is well known that nugget toughness is increased due to the tempering of martensite, hence, promoting pullout failure [16]. As a result, it may be concluded that the increase in the tensile shear load-bearing capability of the welds is caused by tempered martensite that formed within the nugget zone.

3.3. Analysis of Taguchi Signal-to-Noise (S/N) Ratio

Taguchi S/N ratio analysis is the most widely used approach for determining the optimal level of input parameters to produce the optimum quality characteristic [6]. Since the purpose of this work is to produce strong weld joints, the quality feature chosen in this study is "higher is better." Therefore, S/N ratios are computed using the following equation:

$$\left(\frac{signal}{noise}\right) ratio = -10 \log \left(\frac{1}{n} \sum_{i=1}^{n} \frac{1}{y_i^2}\right) \qquad (1)$$

where n denotes the number of experimental trials and, y_i denotes the response value of the ith experiment in the orthogonal array. The value of n is 2 since each experimental run was performed twice.

Fig. 6 shows the S/N ratios graph of tensile shear peak load. The optimal input welding parameters setting for achieving the maximum tensile shear peak load are A4B4C1, i.e., 7.5 kA secondary pulse welding current, 560 ms secondary pulse welding time, and 400 ms first pulse holding time. In addition, the secondary pulse welding current shows the highest S/N ratios value (i.e., 28.28), which indicates its dominant influence on the tensile shear peak load.
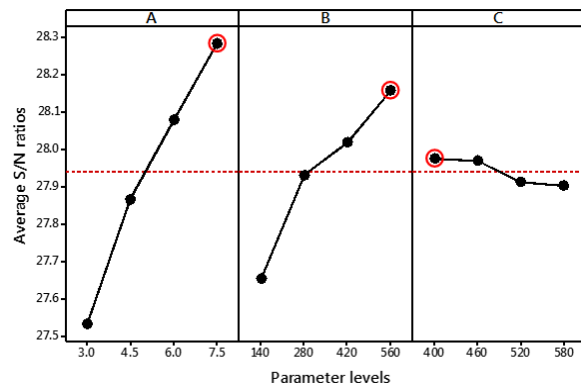

Fig. 6. S/N ratio graph of tensile shear peak load (red circle indicates optimum welding parameters level)

3.4. Confirmation Test

The final step in the design of experiments is to perform the confirmation test. A confirmation test is conducted at the optimum level of input process parameters to verify the estimated value against a confirmed value. In this study, after determining the optimum parameter levels, a new experiment was supposed to be designed to further improve weld quality. It is worth noting that if the optimum parameter levels coincide with one of the experimental runs of OA, then no confirmation test is required [13]. In the present study, a confirmation test is not required because the optimum combination of welding parameters and levels, i.e., A4B4C1, corresponds to experimental run W16.

3.5. Regression Modeling

A mathematical relationship is developed between dependent and independent parameters using a regression method. The tensile shear peak load of the weld joints is the dependent variable in this study, whereas the independent variables are secondary pulse welding current, secondary pulse welding time, and primary pulse holding time. The log-linear model was chosen because it takes the main effects and interactions on transformed variables. The designated general log-linear equation can be expressed as:

$$\ln Y = \beta_0 + \beta_1 A + \beta_2 B + \beta_3 C + \beta_4 AB + \beta_5 AC + \beta_6 BC \quad (2)$$

where, Y is the response variable i.e., tensile shear peak load, β_0 is the response variable at the base level; A is secondary pulse welding current, B is secondary pulse welding time, C is primary pulse holding time, β_1, β_2, β_3 are regression coefficients associated with main process parameters, β_4, β_5, β_6 are parameters interaction coefficients. Minitab®18 software was used to compute the parameter coefficients. After computing each of equation (4)'s coefficients and substituting the coded values of the variables, the log-linear regression equation for predicting the tensile shear peak load can be re-written as follows:

$$\text{TS.Peak Load} = \quad (3)$$
$$e^{(3.594-0.0796A-0.000262B-0.000989C+0.000047AB+0.000173AC+0.000001BC)}$$

Table 5 shows the regression predicted tensile shear peak loads of the welded joints. The adequacy of the regression model is confirmed by using analysis of variance (ANOVA) and Fisher's (F) test. The coefficient of determination (R^2) and adjusted coefficient of determination (adj R^2) are used in ANOVA to assess a model's fitness. In general, the F-value at a given DOF for the regression model and the error are compared at a confidence level of 95%. The model is considered statistically significant if the estimated F-value is higher than the tabulated F-value [18]. Table 5 shows the ANOVA and F-test results of the model. According to ANOVA results, the value of R^2 is 94.75 % and adj R^2 is 91.26% which implies that the model is statistically significant. According to the F-test result, the calculated F-value of the model is 27.09 which is greater than the tabulated F-value i.e., 3.3738, thus regression model is confirmed to be adequate signifies the actual relationship between the input welding process parameters and the response. Furthermore, the F-test is utilized to identify process parameters that have a substantial effect on quality characteristics. An F-value greater than four usually implies that the parameter effect is quite large [13]. It is observed that the F-value of parameters A and C and interactions AB and AC are greater than 4. Thus, the indicated two parameters and two interactions have a significant effect on the tensile shear peak load of weld joints.

Table 5. Analysis of variance and F-test results for tensile shear peak load model

Source	DOF	Sum of squares	Mean square	F-Value	P-Value
Regression model	6	0.026246	0.004374	27.09	0.000
A	1	0.001690	0.001690	10.46	0.010
B	1	0.000147	0.000147	0.91	0.365
C	1	0.001569	0.001569	9.72	0.012
AB	1	0.000853	0.000853	5.28	0.047
AC	1	0.002127	0.002127	13.17	0.005
BC	1	0.000157	0.000157	0.97	0.349
Error/Residual	9	0.001453	0.000161		
Total	15	0.027699			
R-sq= 94.75 %, R-sq(adj)= 91.26 %					
F- value (calculated), f (6,9,0.05)= 27.09, F- value (tabulated), f (6,9,0.05)= 3.3738					

3.6. Artificial Neural Network Modeling

To predict the tensile shear peak load of the welds, the data is modeled using an artificial neural network. Fig. 7 shows the topological structure of the network used in the present investigation.
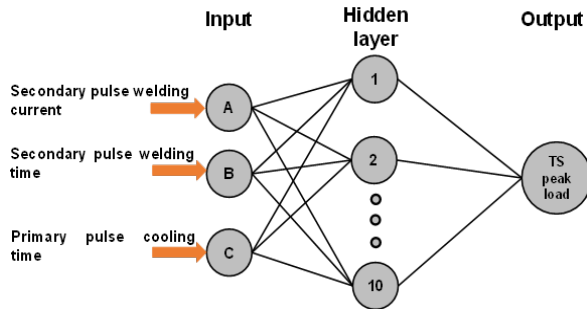

Fig. 7. The ANN topology used for prediction of tensile shear peak load

A feed-forward back propagation (BP) network is used to learn the mapping between inputs parameters (i.e, A, B and C) and output response (i.e, tensile shear peak load). One hidden layer with 10 neurons is used to compute the nonlinear mapping between inputs and output(s). Levenberg-Marquardt (LM) algorithm was used for training the neural networks. The LM algorithm was trained for 6 iterations. The transfer function of the hidden layer was set as the sigmoid function. For the training of the network, 75% of data (twelve experimental runs) are used, and the remaining 30% of data (four experimental runs) are used for testing and validation. The experimental data for training and testing were chosen at random.

The accuracy of the ANN model is checked by using Pearson's correlation coefficient (R). In statistics, the correlation coefficient is a statistical measure of the strength of correlation between experimental vs. estimated value. A correlation coefficient of 1 means there is no error and all points lie on the line passing through the origin. The very high correlation coefficient between experimental and predicted tensile shear peak load for training testing, validation, and all data set confirms the high accuracy of the ANN model, as shown in Fig. 8.
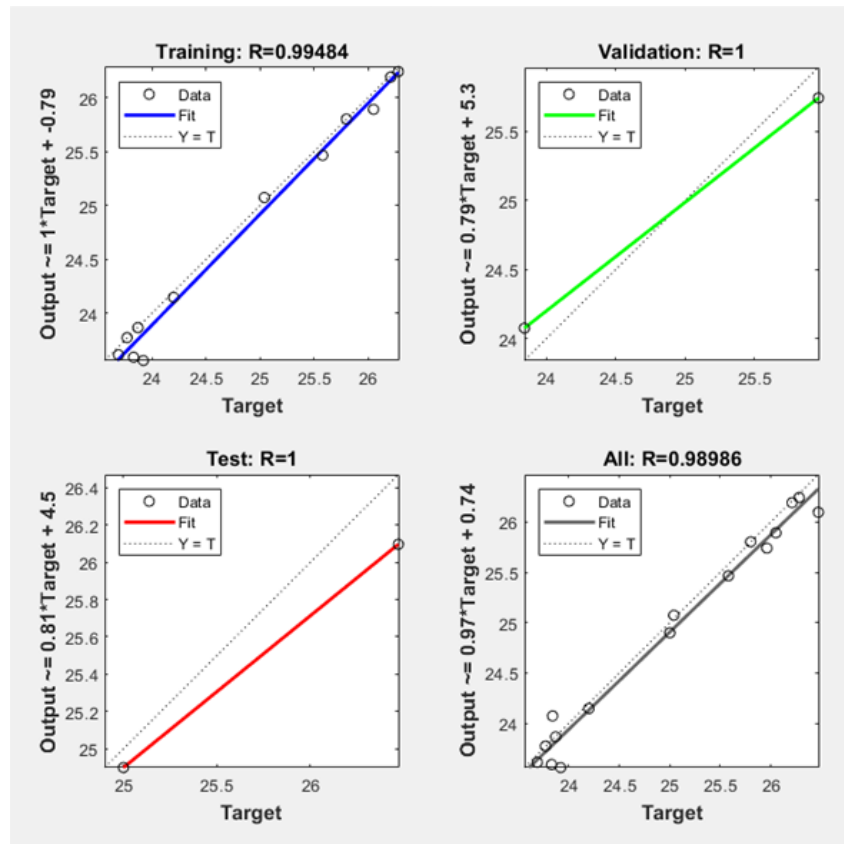

Fig. 8. Analysis of Pearson's correlation coefficient R of the experimental and predicted tensile shear peak load of the welds using ANN model

3.7. Selecting an accurate model

Fig. 9 shows the experimental versus predicted tensile shear peak load and the verified prediction accuracies of the regression model and neural network model. The percentage errors of the models are used to assess the performance. Fig. 10 presents the percentage errors of the two models based on the validation data. It may be argued that the BP neural network outperforms the regression model due to its lower mean value of the error. One of the primary reasons for the BP neural network model's better performance is its random non-linear mapping capability. However, it is proposed that further training data could increase the ANN model's accuracy.
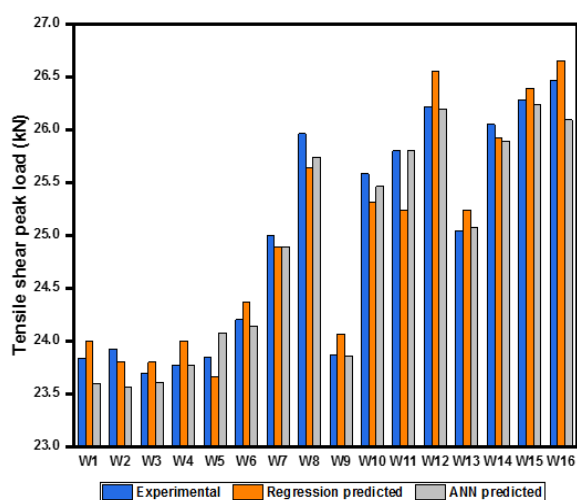

Fig. 9. Tensile shear peak load experimental vs predicted using the regression model and neural network model
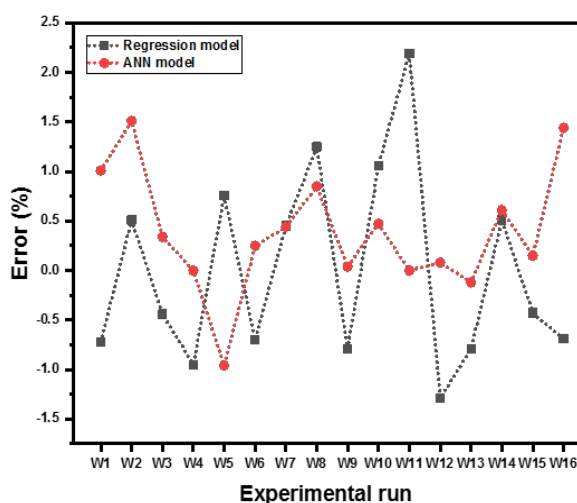

Fig. 10. Comparison of errors in regression and ANN models

4. CONCLUSIONS

This paper presented the investigation of the optimization, modeling, and effect of welding parameters on the tensile shear load-bearing capacity of double pulse resistance spot welded DP590 steel.

Based on the results following conclusions are drawn:

1) A maximum average tensile shear peak load of 26.47 was achieved at optimum welding parameters i.e., second pulse welding current of 7.5 kA, second pulse welding time of 560 ms, and first pulse holding time of 400 ms. Based on S/N ratios, it was found that the second pulse welding current is the most influential parameter that controls the tensile shear load-bearing capacity of the welds.

2) The results also showed that increasing secondary pulse welding current and welding time and decreasing first pulse holding time could lead to weld joints of high load-carrying capacity.

3) The ANN model predicted the output response with high accuracy even with fewer training data. The ANN model showed small percentage error than the regression model.

ACKNOWLEDGMENT

CONFLICT OF INTEREST

The authors declare that they have no financial or non-financial conflict of interest.

DATA AVAILABILITY STATEMENT

The raw/processed data required to reproduce these findings cannot be shared at this time due to technical or time limitations.

REFERENCES

[1] Demeri, M.Y., Dual Phase Steels, Advanced High-Strength Steels: Science, Technology and Applications, ed. M. Y.

Demeri, ASM International, USA, 2013, 95-105.

[2] Soomro, I. A., Pedapati, S. R., and Awang, M., "A Review of Advances in Resistance Spot Welding of Automotive Sheet Steels: Emerging Methods to Improve Joint Mechanical Performance". Int. J. Adv. Manuf. Technol., 2021, 118(5-6):1335-1366.

[3] Chabok, A., Cao, H., van der Aa, E., and Pei, Y., "New Insights Into the Fracture Behavior of Advanced High Strength Steel Resistance Spot Welds". J. Mater. Process. Technol., 2022, 301:117433.

[4] Sajjadi-Nikoo, S., Pouranvari, M., Abedi, A., and Ghaderi, A. A., "In Situ Postweld Heat Treatment of Transformation Induced Plasticity Steel Resistance Spot Welds". Sci. Technol. Weld Join., 2017, 23(1):71-78.

[5] Chabok, A., van der Aa, E., Basu, I., De Hosson, J., and Pei, Y., "Effect of Pulse Scheme on the Microstructural Evolution, Residual Stress State and Mechanical Performance of Resistance Spot Welded DP1000-GI Steel". Sci. Technol. Weld. Join., 2018, 23(8):649-658.

[6] Thakur, A., Rao, T., Mukhedkar, M., Nandedkar, V., "Application of Taguchi method for resistance spot welding of galvanized steel". ARPN. J. Eng. Appl. Sci, 2010, 5(11):22-26, 2010.

[7] Pattanaik, A. K., Pradhan, S., Panda, S. N., Bagal, D. K., Pal, K., and Patnaik, D., "Effect of Process Parameters on Friction Stir Spot Welding Using Grey Based Taguchi Methodology". Mater. Today. Proc., 2018, 5(5):12098-12102.

[8] Tamhane, A.C., Statistical Analysis of Designed Experiments: Theory And Applications. John Wiley & Sons; 2009.

[9] Soomro, A. A., Mokhtar, A. A., Kurnia, J. C., Lashari, N., Lu, H., and Sambo, C., "Integrity Assessment of Corroded Oil and Gas Pipelines Using Machine Learning: A Systematic Review". Eng. Fail. Anal., 2022, 131:105810.

[10] Kannan, T. D. B., Ramesh, T., and Sathiya, P., "Application of Artificial Neural Network Modelling for Optimization of Yb: YAG Laser Welding Of Nitinol". Trans. Indian. Inst. Metals., 2017, 70(7):1763-1771.

[11] Arunchai, T., Sonthipermpoon, K., Apichayakul, P., and Tamee, K., ""Resistance Spot Welding Optimization Based on Artificial Neural Network". Int. J. Manuf. Eng., 2014, 154784.

[12] Babu, K. Kamal et al., "Parameter Optimization of Friction Stir Welding of Cryorolled AA2219 Alloy Using Artificial Neural Network Modeling with Genetic Algorithm". Int. J. Adv. Manuf. Tech, 2018; 94(9):3117-3129.

[13] P. S Rao, O. P Gupta, S. S. N Murty, and A. B. K Rao. "Effect of Process Parameters and Mathematical Model for the Prediction of Bead Geometry in Pulsed GMA Welding". Int.J.Adv Manuf. Technol 2009, 45(5):496-505.

[14] Soomro, I. A., Pedapati, S. R., and Awang, M., "Double Pulse Resistance Spot Welding of Dual Phase Steel: Parametric Study on Microstructure, Failure Mode and Low Dynamic Tensile Shear Properties". Mater., 2021, 14(4):1-19.

[15] Pouranvari, M., Hoveida Marashi, S. P., and Jaber, H. L., "DP780 Dual-Phase-Steel Spot Welds: Critical Fusion-Zone Size Ensuring the Pull-Out Failure Mode". Materiali. Tehnologije., 2015 49(4):579-585.

[16] Aghajani, H., and Pouranvari, M., "Influence of In Situ Thermal Processing Strategies on the Weldability of Martensitic Stainless Steel Resistance Spot Welds: Effect of Second Pulse Current on the Weld Microstructure and Mechanical Properties". Metall Mater Trans A., 2019, 50(11):5191-5209.

[17] Zhao, D., Wang, Y., Liang, D., and Ivanov, M., "Performances of Regression Model and Artificial Neural Network in Monitoring Welding Quality Based on Power Signal". J. Mater. Res Technol, 2020; 9(2):1231-1240.

[18] Montgomery, D.C., Design and Analysis of Experiments, 8th ed. John Wiley & Sons, Inc., 2012.

[19] Kulekci, M. K., Esme, U., Er, O., and Kazancoglu, Y., "Modeling And Prediction of Weld Shear Strength in Friction Stir Spot Welding Using Design Of Experiments and Neural Network. Materialwissenschaft. Werkstofftechnik., 2011, 42(11):990-995.